A Novel Method for Turn to Turn Fault Detection in Shunt Reactors

Sarasij Das[1], Tarlochan Sidhu[2], *Fellow, IEEE,* Mohammad Reza Dadash Zadeh[3] and Zhiying Zhang[4]

[1] Indian Institute of Science, Bangalore, India; [2] University of Ontario Institute of Technology (UOIT), Oshawa, On, Canada; [3] ETAP, Irvine, CA, USA; [4] GE Grid Solutions, Markham, On, Canada

***Abstract*- Turn to turn faults usually cause smaller changes in the phase currents of a shunt reactor when fewer turns are involved. Designing a sensitive and reliable algorithm for turn to turn fault detection in shunt reactors still remains a challenge. In this paper, a novel hybrid differential algorithm has been proposed to detect turn to turn faults in shunt reactors. The proposed algorithm calculates the difference between normalized negative sequence terminal voltage and normalized negative sequence reactor current phasors. This difference value is used for detecting turn to turn fault in shunt reactors. The proposed algorithm can also identify the faulty phase. This is a significant improvement with respect to the existing negative or zero sequence based methods. The proposed algorithm does not need neural CT. Impedance values of the shunt reactors are also not needed in the calculations. The proposed algorithm can be applied to both solidly and impedance grounded shunt reactors. The performance of the proposed algorithm is evaluated using PSCAD simulations. It is found that the proposed algorithm is sensitive enough to detect lower level turn to turn faults. The proposed algorithm performs satisfactorily during system unbalances, reactor energizations, external faults, off-nominal frequency and switch onto fault scenarios, etc.**

***Index Terms*—Fault detection, Power System Protection, Shunt Reactor, Turn to turn fault.**

I. Introduction

Shunt reactors are often used for reducing over-voltages on EHV/HV transmission lines [1][2]. EHV/HV shunt reactors are mostly connected in wye configuration. These reactors are either solidly grounded or impedance grounded. Solidly grounded shunt reactors are most common. Oil-filled gapped iron-core reactor has longer range of linear operation [3][4][5] in comparison to a power transformer. The reactor air gaps lead to very little remanence in contrast to a power transformer [5]. As a result, gapped iron-core reactor experiences less severe inrush in comparison with a transformer. Shunt reactors usually have high X/R ratios.

In a shunt reactor, the insulation between two or more turns fails during turn to turn fault. Turn to turn fault usually causes smaller changes in the phase currents of a shunt reactor. A turn to turn fault may evolve into more serious fault if it is not detected early. However, it is difficult to design a sensitive and reliable protection scheme to detect low level turn to turn faults as the changes in reactor phase currents are comparatively small. Turn to turn fault detection is also an issue in power transformers [6-9], synchronous machines [10], induction machine [11-12], the control winding of a magnetically controlled shunt reactor [13].

During turn to turn fault in a shunt reactor, traditional current differential or negative sequence current differential protection cannot see [2] any change in the differential current as the incoming and outgoing currents are same. Impedance relays are mainly used as back-up protection for the oil-filled shunt reactors [5]. They are not sensitive enough to detect low level turn to turn faults [5]. Impedance relays are usually set at 60% [5] of the rated reactor impedance. In some countries, split phase protection is used for turn to turn fault detection. However, the need of special reactor configuration with built-in CTs creates manufacturing problem [3]. Earth-fault overcurrent protection controlled by directional zero sequence element [2][5] is mostly used in North America for turn to turn fault detection. This scheme cannot identify the faulty phase. In addition, this protection needs neutral CT for operation. Unavailability of enough polarizing zero sequence voltage may cause difficulty in the operation of this scheme. In some cases, directional negative sequence element controlled earth-fault overcurrent protection is also used [2][5]. This scheme needs neutral CT for operation. Also, this scheme cannot identify the faulty phase. Paper [14] uses location of negative sequence impedance in the impedance plane to detect turn to turn fault. This method cannot identify the fault phase. Also, this method may not work if turn to turn fault takes place in pre-existing system unbalance condition. Mechanical fault detection techniques such as Buchholz relays are not sensitive enough [5] to detect low level turn to turn fault.

In this paper, a novel hybrid differential protection algorithm has been proposed to detect turn to turn fault in the wye connected shunt reactors. The proposed algorithm is termed as 'hybrid differential' as it operates on the difference between normalized negative sequence terminal voltage and normalized negative sequence phase current of the reactor. The proposed algorithm is sensitive enough to detect low level turn to turn faults. The faulty phase can be identified in the proposed algorithm. This is a significant improvement over the existing negative or zero sequence based techniques.

II. Proposed Algorithm

A. Solidly Grounded Shunt Reactor

Let us consider a solidly grounded symmetrical shunt reactor as shown in Fig. 1(a). Ignoring mutual coupling between phases, the phase currents can be expressed as:

$$I_A = \frac{V_A}{Z_A};\quad I_B = \frac{V_B}{Z_B};\quad I_C = \frac{V_C}{Z_C} \tag{1}$$

$$\begin{bmatrix} V_0 \\ V_1 \\ V_2 \end{bmatrix} = \frac{1}{3}\begin{bmatrix} 1 & 1 & 1 \\ 1 & a & a^2 \\ 1 & a^2 & a \end{bmatrix}\begin{bmatrix} V_A \\ V_B \\ V_C \end{bmatrix} \qquad where\ a = e^{i\frac{2\pi}{3}} \tag{2}$$

Variables $V_{Neg\_Normalized}$ and $I_{Neg\_Normalized}$ are defined as:

$$V_{Neg\_Normalized} = \frac{V_2}{V_1}\times 100\%\ ;\quad I_{Neg\_Normalized} = \frac{I_2}{I_1}\times 100\% \tag{3}$$

Variables $V_{Neg\_Normalized}$ and $I_{Neg\_Normalized}$ measure the amount of unbalances present in terminal voltages and phase currents respectively. Now, (3) can be written as:

$$V_{Neg\_Normalized} = \frac{V_A + a^2V_B + aV_C}{V_A + aV_B + a^2V_C}\times 100\%$$

$$I_{Neg\_Normalized} = \frac{I_A + a^2I_B + aI_C}{I_A + aI_B + a^2I_C}\times 100\%$$

$$\Rightarrow I_{Neg\_Normalized} = \frac{V_A/Z_A + a^2(V_B/Z_B) + a(V_C/Z_C)}{V_A/Z_A + a(V_B/Z_B) + a^2(V_C/Z_C)}\times 100\% \tag{4}$$

During steady state: $Z_A = Z_B = Z_C = Z$ (5)

Using (5), equation (4) can be re-written as:

$$I_{Neg\_Normalized} = \frac{V_A + a^2V_B + aV_C}{V_A + aV_B + a^2V_C}\times 100\%$$

$$\Rightarrow I_{Neg\_Normalized} = V_{Neg\_Normalized} \tag{6}$$

It is to be noted that the equation (6) is valid for all balanced and unbalanced system voltages. Eq. (6) implies that the current and voltage unbalances are same for a symmetrical shunt reactor when there is no internal fault. It can also be shown that (6) also remains valid when shunt reactor phases have equal mutual coupling between them.

Now, a variable *Diff* is defined to measure the difference between voltage and current unbalances.

$$Diff = V_{Neg\_Normalized} - I_{Neg\_Normalized} \tag{7}$$

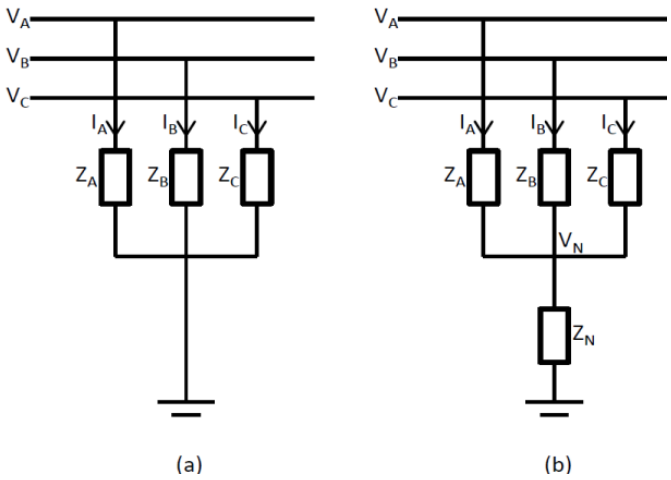

Figure 1: wye-connected solidly and impedance grounded shunt reactors

Suppose, the steady state value of *Diff* is termed as $Diff_{steady}$. From (6), it can be written that:

$$Diff_{steady} = V_{Neg\_Normalized} - I_{Neg\_Normalized} = 0 \tag{8}$$

Now, a turn to turn fault takes place in the phase *B* of the shunt reactor. The decrement in phase *B* impedance is ΔZ_B. In this scenario, $V_{Neg\_Normalized}$ and $I_{Neg\_Normalized}$ can be written as:

$$V_{Neg\_Normalized} = \frac{V_A + a^2V_B + aV_C}{V_A + aV_B + a^2V_C}\times 100\% \tag{9}$$

$$I_{Neg\_Normalized} = \frac{V_A + a^2\left(\frac{V_B}{1-\frac{\Delta Z_B}{Z}}\right) + aV_C}{V_A + a\left(\frac{V_B}{1-\frac{\Delta Z_B}{Z}}\right) + a^2V_C}\times 100\% \tag{10}$$

So, during turn to turn fault:

$$V_{Neg\_Normalized} \neq I_{Neg\_Normalized} \tag{11}$$

$$Diff \neq 0 \tag{12}$$

From the above equations, it can be said that a turn to turn fault causes change in the *Diff* value. This change can be used to detect turn to turn fault in the shunt reactor. To measure the change in *Diff*, a variable *Operate* is defined as:

$$Operate = \left|Diff - Diff_{steady}\right| = \left|Diff - 0\right| = \left|Diff\right| \tag{13}$$

During turn to turn fault, following condition will be valid:

$$Operate > c \tag{14}$$

where, c is a threshold in %.

B. Impedance Grounded Shunt Reactor

The phase currents of an impedance grounded shunt reactor can be expressed as:

$$I_A = \frac{V_A - V_N}{Z_A}; \quad I_B = \frac{V_B - V_N}{Z_B}; \quad I_C = \frac{V_C - V_N}{Z_C} \tag{15}$$

During steady state: $Z_A = Z_B = Z_C = Z$

So, $I_{Neg\_Normalized}$ can be written as:

$$\begin{aligned} I_{Neg\_Normalized} &= \frac{(V_A - V_N) + a^2(V_B - V_N) + a(V_C - V_N)}{(V_A - V_N) + a(V_B - V_N) + a^2(V_C - V_N)} \times 100\% \\ &= V_{Neg\_Normalized} \end{aligned} \tag{16}$$

So, value of $Diff_{steady}$ for impedance grounded shunt reactor is:

$$Diff_{steady} = V_{Neg\_Normalized} - I_{Neg\_Normalized} = 0 \tag{17}$$

Now, a turn to turn fault takes place in the phase B of the shunt reactor. The decrement in phase B impedance is ΔZ_B. In this scenario, $V_{Neg\_Normalized}$ and $I_{Neg\_Normalized}$ can be written as:

$$V_{Neg\_Normalized} = \frac{V_A + a^2 V_B + a V_C}{V_A + a V_B + a^2 V_C} \times 100\%$$

$$I_{Neg\_Normalized} = \frac{I_A + a^2 I_B + a I_C}{I_A + a I_B + a^2 I_C} \times 100\%$$

$$= \frac{V_A - V_N + a^2\left(\frac{V_B - V_N}{1 - \frac{\Delta Z_B}{Z}}\right) + a(V_C - V_N)}{V_A - V_N + a\left(\frac{V_B - V_N}{1 - \frac{\Delta Z_B}{Z}}\right) + a^2(V_C - V_N)} \times 100\%$$

$$= \frac{V_A + a^2\left(\frac{V_B}{1 - \frac{\Delta Z_B}{Z}}\right) + aV_C - \left(\frac{a^2 \frac{\Delta Z_B}{Z} V_N}{1 - \frac{\Delta Z_B}{Z}}\right)}{V_A + a\left(\frac{V_B}{1 - \frac{\Delta Z_B}{Z}}\right) + a^2 V_C - \left(\frac{a \frac{\Delta Z_B}{Z} V_N}{1 - \frac{\Delta Z_B}{Z}}\right)} \times 100\% \tag{18}$$

So, during turn to turn fault:

$$V_{Neg\_Normalized} \neq I_{Neg\_Normalized}$$

In this case also, $Diff$ differs from $Diff_{steady}$ during turn to turn fault. As a result, equations (13) and (14) can also be used for turn to turn fault detection in the impedance grounded shunt reactor.

C. Phase Selection

Once the presence of turn to turn fault is detected, phase selection algorithm is applied to identify the faulted phase. In the proposed algorithm, phase selection is done based on the value of the angle $Diff_{angle}$ defined as:

$$Diff_{angle} = \angle(Diff - Diff_{steady}) \tag{19}$$

In the proposed algorithm, phase selection criteria are same for the impedance and solidly grounded shunt reactors. In the following section, mathematical formulations are presented for solidly grounded shunt reactors. Formulations for impedance grounded shunt reactors can also be achieved in similar way.

1) Turn to turn fault in Phase B

Suppose, there is a turn to turn fault in the phase B of the solidly grounded shunt reactor.

$$\begin{aligned} Diff_{angle} &= \angle(V_{Neg\_Normalized} - I_{Neg\_Normalized} - Diff_{steady}) \\ &= \angle\left(\frac{V_2}{V_1} - \frac{V_A + a^2\left(\frac{V_B}{1 - \frac{\Delta Z_B}{Z}}\right) + aV_C}{V_A + a\left(\frac{V_B}{1 - \frac{\Delta Z_B}{Z}}\right) + a^2 V_C}\right) \\ &= \angle\left(\frac{V_2}{V_1} - \frac{V_A + a^2 V_B(1 + \frac{\Delta Z_B}{Z} + \left(\frac{\Delta Z_B}{Z}\right)^2 + ...) + aV_C}{V_A + aV_B(1 + \frac{\Delta Z_B}{Z} + \left(\frac{\Delta Z_B}{Z}\right)^2 + ...) + a^2 V_C}\right) \end{aligned} \tag{20}$$

Eq. (20) is obtained using Taylor series. Angle of ΔZ_B is equal to the angle of Z when fault resistance is zero. In addition, ΔZ_B is usually much smaller than the phase impedance Z. So ignoring 2nd and higher order terms of $\Delta Z_B/Z$, (20) can be re-written as:

$$\begin{aligned} Diff_{angle} &\approx \angle\left(\frac{V_2}{V_1} - \frac{V_A + a^2 V_B(1 + \frac{\Delta Z_B}{Z}) + aV_C}{V_A + aV_B(1 + \frac{\Delta Z_B}{Z}) + a^2 V_C}\right) \\ &\approx \angle\left(\frac{V_2}{V_1} - \frac{V_2 + a^2 V_B \frac{\Delta Z_B}{Z}}{V_1 + aV_B \frac{\Delta Z_B}{Z}}\right) \\ &\approx \angle\left(\frac{aV_B \Delta Z_B}{Z}\left(\frac{V_2}{V_1} - a\right) \Big/ \left(V_1 + aV_B \frac{\Delta Z_B}{Z}\right)\right) \\ &\approx \angle\left(-\frac{a^2 V_B \Delta Z_B}{Z\left(V_1 + aV_B \frac{\Delta Z_B}{Z}\right)}\right), \qquad as \left|\frac{V_2}{V_1}\right| << |\alpha| \end{aligned} \tag{21}$$

From the mathematical expression of V_1 it can be said that the angle of V_1 is nearly equal to the angle of V_A. Angle of ΔZ_B is equal to the angle of Z when fault resistance is zero. Angle

of (aV_B) is nearly equal to angle of V_A. As a result, angle of ($V_1 + (aV_B\Delta Z_B/Z)$) is nearly equal to the angle of V_A. So,

$$Diff_{angle} \approx \angle - a \approx -60^0 \quad (22)$$

2) Turn to turn fault in Phase A

Suppose, there is a turn to turn fault in the phase A of the shunt reactor. Following previous steps, we can derive:

$$Diff_{angle} \approx \angle\left(\frac{V_2}{V_1} - \frac{V_2 + V_A\frac{\Delta Z_A}{Z}}{V_1 + V_A\frac{\Delta Z_A}{Z}}\right) \approx \angle\left(-\frac{V_A\Delta Z_A}{Z\left(V_1 + V_A\frac{\Delta Z_A}{Z}\right)}\right), \quad as \left|\frac{V_2}{V_1}\right| << 1 \approx 180^0 \quad (23)$$

3) Turn to turn fault in Phase C

Suppose, there is a turn to turn fault in the phase C of the shunt reactor. Following previous steps, we can derive:

$$Diff_{angle} \approx \angle\left(\frac{V_2}{V_1} - \frac{V_2 + aV_C\frac{\Delta Z_C}{Z}}{V_1 + a^2V_C\frac{\Delta Z_C}{Z}}\right) \approx \angle\left(-\frac{aV_C\Delta Z_C}{Z\left(V_1 + a^2V_C\frac{\Delta Z_C}{Z}\right)}\right), \quad as \left|\frac{aV_2}{V_1}\right| << 1 \approx 60^0 \quad (24)$$

D. Practical Implementation Issues

1) Choice of Threshold c

Threshold c impacts the performance of the proposed algorithm. Threshold c should be chosen such that:

$$c_1 \times SF < c < c_2 \times SF \quad (25)$$

where, c_1 is the maximum value of *Operate* to avoid false tripping during normal operating conditions. And, c_2 is the maximum value of *Operate* to detect minimum level turn to turn fault as per design goal. Value of safety factor *SF* is a choice by the designer. However, value of *SF* should be greater than 1.

An example is given next to show the calculation steps for c_1.

As per [19], the maximum value of normal system voltage unbalance is 2%. So,

$$\left|\frac{V_2}{V_1}\times 100\%\right|_{\max} = 2\ \%$$

$V_{Neg\_Normalized}$ and $I_{Neg\_Normalized}$ can have following values in the 2% system voltage unbalance scenario:

$$V_{Neg\_Normalized} = 2+\mathrm{i}\times 0\ (\%)$$
$$I_{Neg\_Normalized} = 2+\mathrm{i}\times 0\ (\%)$$

Now suppose,

Maximum expected measurement errors = ±5% of actual measurement

So, in a worst case scenario:

$$V_{Neg\_Normalized} = 2\times 1.05+\mathrm{i}\times 0 = 2.1\ (\%)$$
$$I_{Neg\_Normalized} = 2\times 0.95+\mathrm{i}\times 0 = 1.9\ (\%)$$

In this case, c_1 can be chosen as:

$$c_1 = |2.1-1.9| = 0.2\%$$

The calculation steps for c_2 are given below.

Suppose, the design goal is to detect turn to turn faults involving minimum 1.5 % of reactor phase impedance.

Suppose, in steady state scenario:

$$V_A = 1\angle 0^0;\ V_B = 1\angle -120^0;\ V_C = 1\angle 120^0;\ (\text{in p.u})$$
$$Z_A = 0.05 + i\times 1;\ Z_B = 0.05 + i\times 1;\ Z_C = 0.05 + i\times 1;\ (\text{in p.u})$$

Turn to turn fault takes place in phase A of the shunt reactor involving 1.5% reactor phase impedance. Fault resistance is assumed to be zero in this case. So, during turn to turn fault:

$$V_A = 1\angle 0^0;\ V_B = 1\angle -120^0;\ V_C = 1\angle 120^0;$$
$$Z_A = 0.985\times(0.05 + i\times 1);\ Z_B = 0.05 + i\times 1;\ Z_C = 0.05 + i\times 1;$$

Using above phase voltages and impedances:

$$|Diff - Diff_{steady}| = |\ -0.5051+\mathrm{i}\times 0 - 0| = 0.5051\%$$

In this case, c_2 can be chosen as: $c_2 = 0.51\%$

2) Phase Selection

Equations (22), (23) and (24) are derived using many assumptions. The assumptions made behind (22), (23) and (24) may not be valid always. So for practical implementations, a tolerance of ±30° is suggested around the angle values of (22), (23) and (24). Table 1 summarizes the proposed phase selection rules.

Table 1: Phase selection for turn to turn fault detection

$Diff_{angle}$	Phase section decision
$150° \le Diff_{angle} \le 210°$	Turn to turn fault in *phase A*

$270° \le Diff_{angle} \le 330°$	Turn to turn fault in *phase B*
$30° \le Diff_{angle} \le 90°$	Turn to turn fault in *phase C*

3) Impact of Bad Measurements

Adverse impact of bad measurements can be minimized by averaging the values of *Diff* over a specific time. In the proposed algorithm, values of *Diff* are averaged over one cycle. $Diff^{avg}$ is the averaged value of *Diff*. Suppose, the relay runs *p* protection passes per cycle, at the n^{th} protection pass:

$$Diff^{avg}(n) = \frac{1}{p}\sum_{k=1}^{p} Diff(n+1-k) \tag{26}$$

In the proposed algorithm, $Diff^{avg}$ is used instead of *Diff* during calculation of *Operate*. To minimize the impact of bad measurements, the variable *Operate* is calculated as:

$$Operate = \left| Diff^{avg} - Diff_{steady} \right| \tag{27}$$

As a result, $Diff_{angle}$ is calculated as:

$$Diff_{angle} = \angle(Diff^{avg} - Diff_{steady}) \tag{28}$$

4) Declaration of Turn to Turn Fault

In the proposed algorithm, turn to turn fault is declared if the condition (14) is satisfied for specific time duration continuously. This waiting time should be small enough to achieve fast tripping of the shunt reactor during turn to turn fault. However, the waiting time can be comparatively large if the purpose of turn to turn fault protection is to issue an alarm.

5) CT and Reactor Saturations

Digital relays often use CT saturation detector [2][5] or additional time delay [3][5] to avoid maloperation during CT saturations. In the proposed algorithm, waiting time can be made longer enough to cover worst case CT saturation scenarios. Alternately, CT saturation detector can be used to block the proposed algorithm during CT saturations. Similar approaches can be taken to handle reactor saturations in the proposed algorithm.

6) Phase Selection

The proposed algorithm will also respond to other internal faults such as earth and phase-to-phase faults. The phase selection algorithm should be blocked if other protection elements such as earth-fault, differential protection element pick up.

7) Manufacturing Asymmetry between Phases

Ideally, all three phases of a shunt reactor should have same impedance. But in reality, there is always a small amount of asymmetry between the phase impedances of the shunt reactor. Also, reactor phases may have unequal mutual impedances. As per the IEEE Std C57.21-2008 [15], the maximum deviation of impedance in any of the phase shall be within ±2% of the average impedance of the three phases. Practical shunt reactors usually have much lesser asymmetry than specified in the standard [15]. As per [3], the usual value of manufacturing asymmetry is around 0.5%. In the proposed algorithm, $Diff_{steady}$ will have non-zero value for an asymmetrical shunt reactor. Due to asymmetry, the value of $Diff_{steady}$ will also depend on the terminal voltages. $Diff_{steady}$ can be measured at the rated voltages. In addition, the value of $Diff_{steady}$ may change with time due to the ageing of the shunt reactor. So, $Diff_{steady}$ should be updated at regular intervals.

Fig. 2 summarizes the proposed algorithm. The proposed algorithm is termed as 'hybrid differential' as it operates on the difference between normalized negative sequence terminal voltage and normalized negative sequence phase current of the shunt reactor.

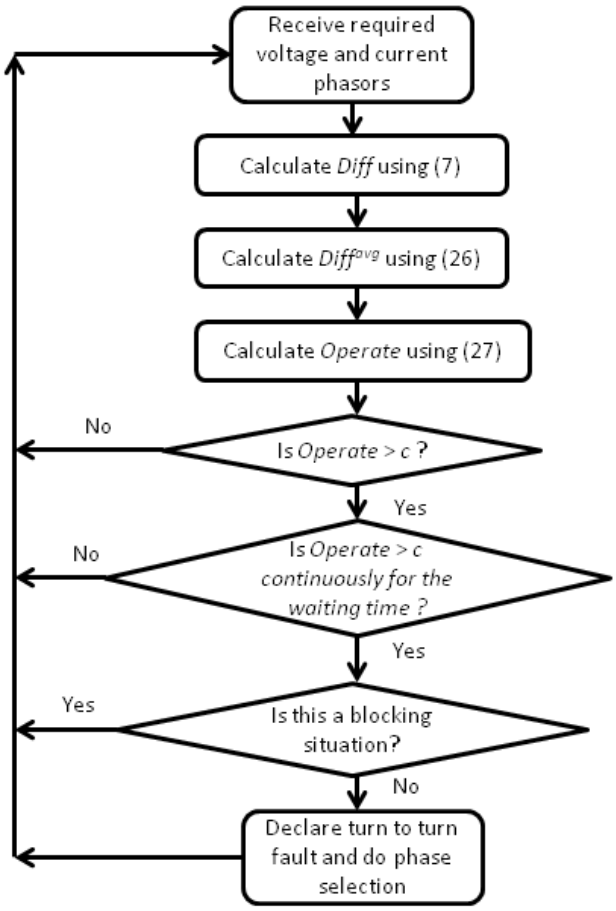

Figure 2: Flow chart of the proposed algorithm

III. Performance Evaluations

The performance of the proposed algorithm has been evaluated using a two bus system as shown in Fig. 3. System voltage is 230 kV and system frequency is 60 Hz unless specified. In Fig. 3, a solidly grounded wye-connected shunt reactor is connected at Bus 1. Unbalanced load is connected at Bus 2 to introduce unbalance in the system voltages. Harmonic current source is connected at Bus 1 to inject small amount of steady state harmonic current into the system. This system has been simulated in PSCAD software. The transmission line is 400 km long. The parameters of transmission line and

generators are taken from [16]. The parameters of load and harmonic current source are given in the Appendix.

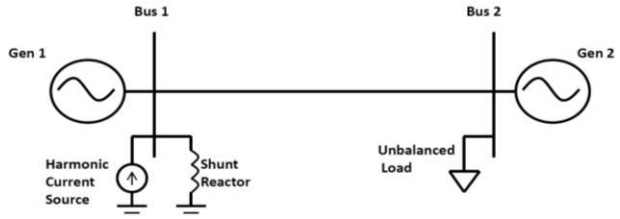

Figure 3: Two bus system with shunt reactor

The proposed algorithm needs voltage and current measurements as inputs. Measurements are generated in PSCAD by the following steps mentioned in [17]. In PSCAD, voltage and current signals are sampled at 20 kHz by selecting an appropriate time-step. The sampled waveforms are then digitally filtered with a second order Butterworth anti-aliasing filter. After anti-aliasing filtering; voltage and current signals are down-sampled to achieve 3840 samples/s sampling rate. Finally, CVT transient, mimic and phasor estimation filters are used to calculate the voltage and current phasors. The protection pass is considered to be 960 sample/s. The value of the threshold c is 0.25 %. Shunt reactors are modeled as saturable reactors. The magnetizing characteristic of saturable reactor is taken from [5]. Report [5] says that the knee point of typical gapped code oil immersed shunt reactor falls in the 1.25 pu to 1.35 pu range. In this study, knee point is chosen as 1.35 pu. The X/R ratio of unsaturated reactor phase impedance is 100. The per-phase reactance of shunt reactor is 1000 Ω. Reactor phase voltage and phase current phasors contain 50 dB noises. Total Harmonic Distortion in phase currents is around 0.15%. Steady state system voltage unbalance is around 0.2%. $Diff_{steady}$ is zero in all the simulations. In these simulations, a waiting time of 0.5 s is used before turn to turn fault is declared.

A. Performance during turn to turn fault

Suppose, turn to turn fault takes place in the phase A of the shunt reactor involving 1.5% reactor impedance. The fault starts at 3 s and fault resistance is 1 Ω. Fig. 4 shows the effect of turn to turn fault on the phase voltages and currents. The phase voltages remain almost same as the level of turn to turn fault is low. In Fig. 4, phase A current increases due to the turn to turn fault. In Fig. 5, trajectory of $Diff^{avg}$ - $Diff_{steady}$ is presented in polar coordinates. Initially, the operating point lies within the threshold circle of radius 0.25%. However, the operating point crosses the threshold circle after turn to turn fault starts. The operating point settles outside the threshold circle. As a result, turn to turn fault is declared after waiting for 0.5 s. Phase selection algorithm finds that the value of $Diff_{angle}$ remains around 180 degrees during turn to turn fault. As a result, turn to turn fault is declared in phase A. Fig. 6 & 7 show the performance of the proposed algorithm during off-nominal frequency. The system frequency is 59.5 Hz. A turn to turn fault takes place in the phase A of the shunt reactor involving 1.5% of phase impedance. In Fig. 7, trajectory of $Diff^{avg}$ - $Diff_{steady}$ is presented in polar coordinates. In this case also, the proposed algorithm performs satisfactorily. In this paper, frequency tracking has not been used during phasor estimations. As a result, voltage and current phasors of Fig. 6 have more estimation errors than the phasors of Fig. 4. Fig. 7 shows that the performance of proposed algorithm does not get affected much during off-nominal frequencies. This happens due to the averaging of $Diff$ values over one cycle.

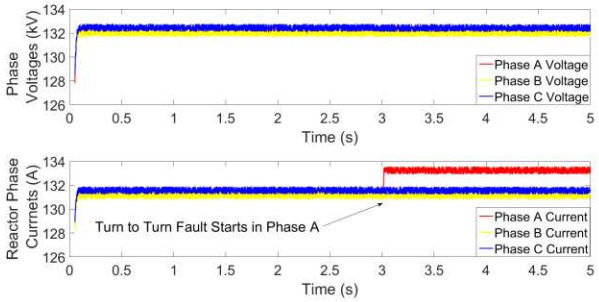

Figure 4: Phase voltages and currents during turn to turn fault in phase A (system frequency 60 Hz)

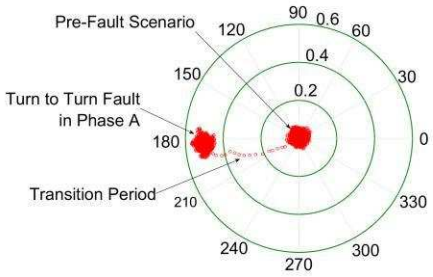

Figure 5: Trajectory of $Diff^{avg}$ - $Diff_{steady}$ in polar coordinates corresponding to Figure 4

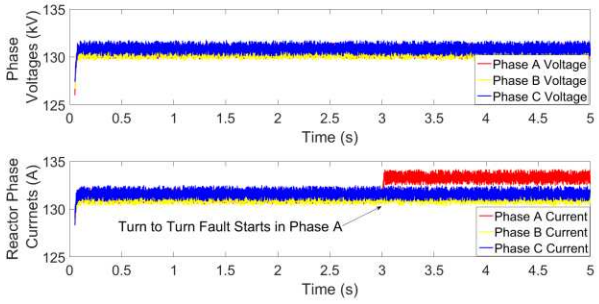

Figure 6: Phase voltages and currents during turn to turn fault in phase A (system frequency 59.5 Hz)

Fig. 8 presents the effect of noises on the phase selection performance. In Fig. 8, polar plot of $Diff^{avg}$ - $Diff_{steady}$ is presented for 100 phase selection instances with varying amounts of noises. All other simulation parameters remain same. Each point on Fig. 8 presents the value of $Diff^{avg}$ - $Diff_{steady}$ corresponding to the time instant when turn to turn fault is declared. In all the 100 runs, the values of $Diff_{angle}$ remain within the phase selection zone of phase A. The phase selection algorithm performs satisfactorily in this case.

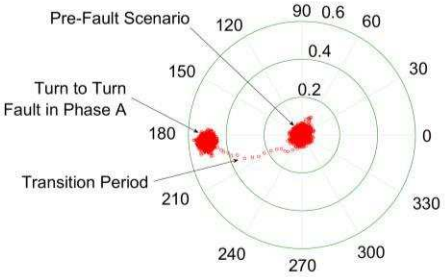

Figure 7: Trajectory of $Diff^{avg}$ - $Diff_{steady}$ in polar coordinates corresponding to Figure 6

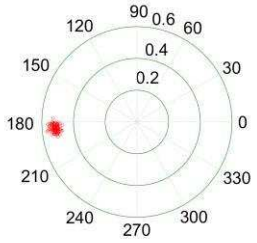

Figure 8: Polar plot of $Diff^{avg}$ - $Diff_{steady}$ for 100 phase selection instances with varying noises and turn to turn fault in phase A

B. Performance during external fault

In this section, the performance of the proposed algorithm is evaluated for an external A-G fault. The A-G fault is located at the center of the transmission line. Single pole tripping of phase A takes place after 0.1 s of fault starting. Phase A breaker recloses after 0.75 s dead time [18]. It is assumed that the fault was temporary in nature. As a result, fault disappeared during dead time and phase A of the transmission line gets successfully reclosed. There is no simultaneous turn to turn fault in the shunt reactor. Phase currents of the transmission line are presented in Figure 9.

Performance of the proposed algorithm is presented Figure 10. In Fig. 10, variable *Operate* stays below the threshold value except momentary jumps. These momentary jumps appear due to the errors in phasor estimations during transition periods. The time durations of momentary jumps depends on the response time of the estimation filter. As a result, durations of the momentary jumps are much smaller than the waiting time. The proposed algorithm does not detect turn to turn fault scenario as expected.

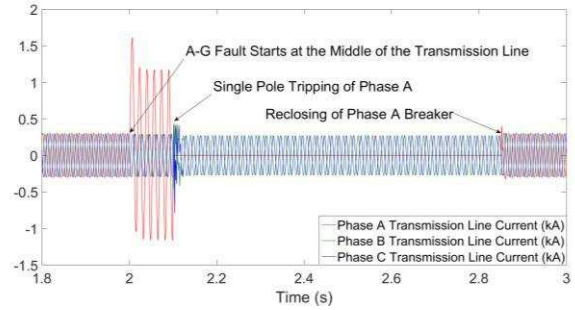

Figure 9: Phase currents of the transmission line

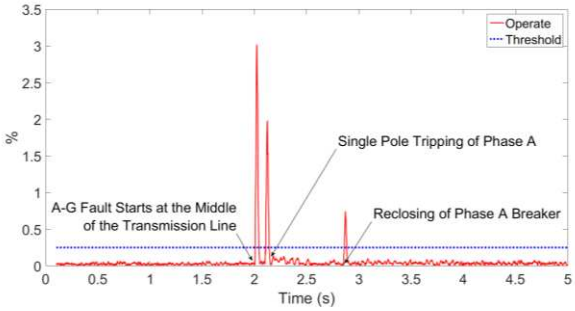

Figure 10: External A-G fault with single pole tripping and auto-reclosing

Fig. 11 presents the performance of the phase selection algorithm during external fault with simultaneous turn to turn fault in phase *C*. In Fig. 11, polar plot of $Diff^{avg}$ - $Diff_{steady}$ is presented for 100 phase selection instances with varying amounts of noises. The phase selection algorithm performs satisfactorily in this case.

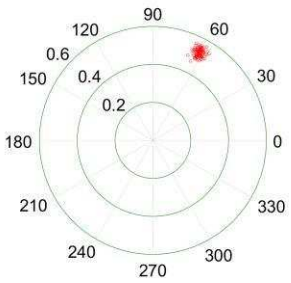

Figure 11: Polar plot of $Diff^{avg}$ - $Diff_{steady}$ for 100 phase selection instances with varying noises and external fault with simultaneous turn to turn fault in phase *C*

C. Performance during shunt reactor energization

In Fig. 12 and 13, the performance of the proposed algorithm during shunt reactor energization is presented. Breakers in all the three phases are closed together at 1 s. There is no synchronized switching of the reactor. Figure 12 presents the CT secondary currents corresponding to the energization event. After energization, phase A of the reactor saturates. Phase A current comes out of the saturation after 4 cycles approximately. Phase B and C do not saturate but contain decaying DC components. There is no simultaneous turn to turn fault in the shunt reactor. Fig. 13 presents the performance of the proposed algorithm during shunt reactor

energization. After energization, the value of *Operate* goes above the threshold for 5 cycles approximately and then it falls and settles below the threshold. As expected, the proposed algorithm does not detect turn to turn fault scenario.

In Fig. 14, the performance of the proposed algorithm is presented for turn to turn fault happening in phase *B* during reactor energization. In this case, the value of *Operate* stays above the threshold value continuously for more than 0.5 s. The value of $Diff_{angle}$ remains around -53 degrees. As a result, turn to turn fault is declared in phase *B*.

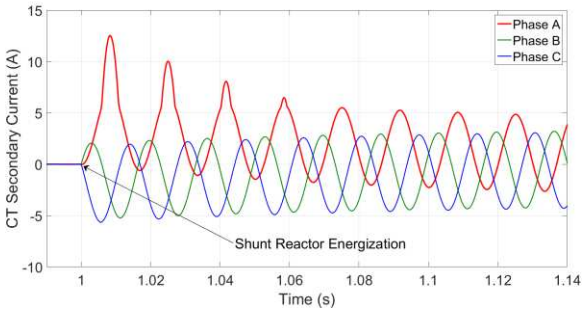

Figure 12: CT secondary current (A) during shunt reactor energization

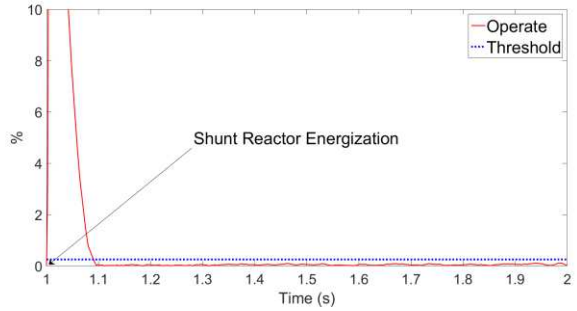

Figure 13: Shunt reactor energization without simultaneous turn to turn fault

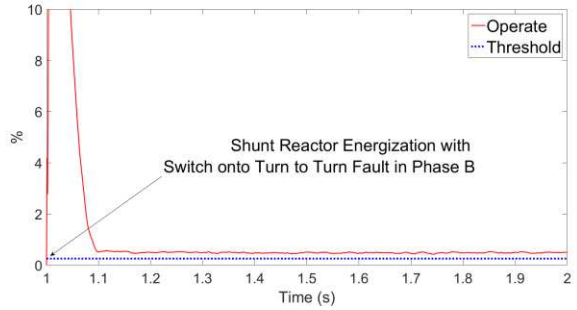

Figure 14: Shunt reactor energization with switch onto turn to turn fault in phase *B*

D. Performance during high level turn to turn faults

In this section, the performance of the proposed algorithm has been evaluated for higher level turn to turn faults. A turn to turn fault takes place in the phase *A* of a shunt reactor involving 50% of the phase impedance. In Fig. 15, the trajectory of $Diff^{avg}$ - $Diff_{steady}$ is presented in polar coordinates. Fig. 15 shows that the proposed algorithm correctly detects presence of turn to turn fault in phase A. In practical scenario, other protection elements (51N, 21, etc.) will respond to such higher level turn to turn fault and will cause tripping at much earlier time. The proposed hybrid differential algorithm can be used as a backup protection in such case.

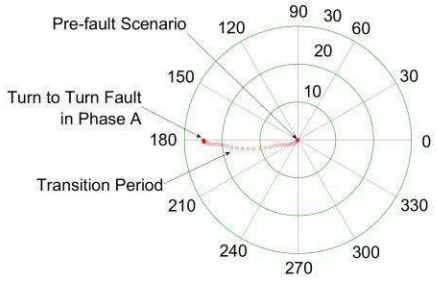

Figure 15: Trajectory of $Diff^{avg}$ - $Diff_{steady}$ in polar coordinates during turn to turn fault in phase A involving 50% of the phase impedance

E. Asymmetry in the reactor phase impedances

In this study, the phase *B* impedance is 100.5% of the phase A impedance and the phase *C* impedance is 99.5% of the phase A impedance. A turn to turn fault takes place in the phase A of the shunt reactor involving 1.5% of the phase impedance. Fig. 16 shows the corresponding trajectory of $Diff^{avg}$ - $Diff_{steady}$. The proposed algorithm performs correctly in this case.

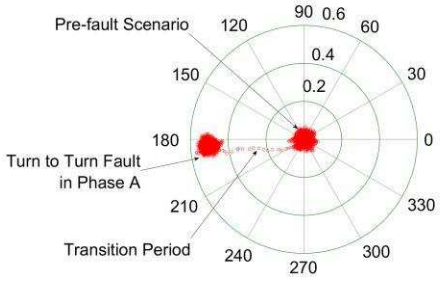

Figure 16: Trajectory of $Diff^{avg}$ - $Diff_{steady}$ during turn to turn fault in phase A of an asymmetrical shunt reactor

F. Performance comparison

Negative sequence current differential element [7] is commonly used for turn to turn fault detection in power transformers. In this section, the performance of the proposed algorithm is compared with the method [7]. There is a turn to turn fault in phase A of the reactor at 3 s. Negative sequence differential current is measured using CTs located at the both ends of the shunt reactor windings. Fig. 17 presents the magnitudes of negative sequence differential currents along with the values of *Operate*. The proposed algorithm satisfactorily detect turn to turn fault. However, from Fig. 17 it is evident that the negative sequence current differential element fails to detect turn to turn fault. This is expected as the incoming and outgoing negative sequence currents are same during turn to turn fault. The proposed method

demonstrates superior performance with respect to the negative sequence current differential element.

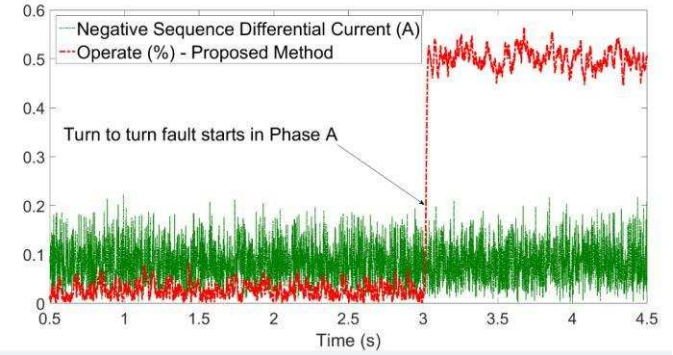

Figure 17: Performance comparison with Negative Sequence Current Differential element

IV. Conclusions

In this paper, a novel hybrid differential algorithm has been proposed to detect turn to turn fault in the shunt reactors. The proposed algorithm can identify the faulty phase. This is a significant improvement over the existing negative/zero sequence based techniques. Impedance values of the shunt reactors are not needed in the calculations. The proposed algorithm works for both solidly grounded and impedance grounded shunt reactors and does not need a neutral CT. Results demonstrate that the proposed algorithm performs satisfactorily during system unbalances, external faults and reactor energization scenarios. The proposed algorithm can also detect switch onto turn to turn faults. The proposed algorithm is sensitive enough to detect both low and high level turn to turn faults.

V. Appendix

Impedances of the unbalanced load:
Z_{AL}=600 Ω; Z_{BL}=800 Ω; Z_{CL}=1000 Ω

Harmonic current source:
Frequency = 180 Hz; Magnitude = 0.01 kA

VI. Acknowledgement

The authors gratefully thank Ilia Voloh of the GE Grid Solutions for his feedback on this work.

VII. References

[1] E. Nashawati, N. Fischer, B. Le, and D. Taylor, “Impacts of Shunt Reactors on Transmission Line Protection,” *in proceedings 38th Annual Western Protective Relay Conference*, Spokane, WA, October 2011.

[2] Basha, Faridul Katha, and Michael Thompson. "Practical EHV reactor protection." *in proceedings 66th Annual Conference for Protective Relay Engineers*, College Station, TX 2013, pp. 408 - 419.

[3] Gajić, Zoran, Birger Hillström, and Fahrudin Mekić. "HV shunt reactor secrets for protection engineers." *in proceedings 30th Western Protective Relaying Conference*, Washington. 2003.

[4] *IEEE Guide for the Protection of Shunt Reactors*, IEEE Std C37.109-2006, Dec. 2006.

[5] *Protection, Monitoring and Control of Shunt Reactors,* CIGRE Report 546, Working Group B5.37, August 2013

[6] Zacharias, Daniel, and Ramakrishna Gokaraju. "Prototype of a Negative-Sequence Turn-to-Turn Fault Detection Scheme for Transformers." *IEEE Transactions on Power Delivery*, vol. 31, no. 1, pp. 122-129, Feb. 2016.

[7] Z. Gajić, I. Brnčić, B. Hillström, and I. Ivankovic, “Sensitive turn-to-turn fault protection for power transformers,” presented at the CIGRÉ Study Committee B5 Colloq., Calgary, AB, Canada, 2005

[8] Abu-Siada, Ahmed, and Syed Islam. "A novel online technique to detect power transformer winding faults." *IEEE Transactions on Power Delivery*, vol. 27, no. 2, pp. 849-857, Jan. 2012.

[9] Ballal, MS, HM Suryawanshi, M K. Mishra, and BN Chaudhari. "Interturn Faults Detection of Transformers by Diagnosis of Neutral Current." *IEEE Transactions on Power Delivery*, vol. 31, no. 3, pp 1096-1105. Jun. 2016.

[10] Nyanteh, Y., Edrington, C., Srivastava, S. and Cartes, D., “Application of artificial intelligence to real-time fault detection in permanent-magnet synchronous machines”. *IEEE Transactions on Industry Applications*, vol. 49, no. 3, pp.1205-1214, May/June 2013.

[11] S Jeevanand, Bhim Singh, and B K Panigrahi. "Incipient turn fault detection and condition monitoring of induction machine using analytical wavelet transform." *IEEE Transactions on Industry Applications*, vol. 50, no. 3, pp 2235-2242, May-June 2014.

[12] Lee, SB, R M. Tallam, and TG. Habetler. "A robust, on-line turn-fault detection technique for induction machines based on monitoring the sequence component impedance matrix." *IEEE Transactions on Power Electronics*, vol 18, no. 3, pp 865-872, May 2003.

[13] Zheng, Tao, Y J. Zhao, et al. "Design and Analysis on the Turn-to-Turn Fault Protection Scheme for the Control Winding of a Magnetically Controlled Shunt Reactor." *IEEE Transactions on Power Delivery*, vol. 30, no. 2, pp. 967-975, April 2015.

[14] Kasztenny, Bogdan, Normann Fischer, and Héctor J. Altuve. "Negative-sequence differential protection-principles, sensitivity, and security." *in proceedings 68th Annual Conference for Protective Relay Engineers,* pp. 364-378, Apr. 2015.

[15] *IEEE Standard Requirements, Terminology, and Test Code for Shunt Reactors Rated Over 500 kVA*, IEEE Std C57.21-2008, Mar. 2008.

[16] Brahma, S.M., and Adly A. Girgis. "Fault location on a transmission line using synchronized voltage measurements." *IEEE Transactions on Power Delivery*, vol. 19, vol. 4, pp. 1619-1622, Oct. 2004.

[17] Brahma, Sukumar M., Phillip L. De Leon, and Rajesh G. Kavasseri. "Investigating the option of removing the antialiasing filter from digital relays." *IEEE Transactions on Power Delivery*, vol. 24, no. 4, pp. 1864-1868, Oct. 2009.

[18] F.Zhalefar, " Adaptive Single-Phase Reclosing in Transmission Lines," Ph.D. dissertation, Electrical and Computer Engineering, Univ. of Western Ontario, 2015.

[19] Von Jouanne, Annette, and Basudeb Banerjee. "Assessment of voltage unbalance." Power Delivery, IEEE Transactions on 16.4 (2001): 782-790.

VIII. Biographies

Sarasij Das is currently working as an assistant professor at the Indian Institute of Science, Bangalore, India.

Tarlochan S. Sidhu (M’90 – SM’94 – F’04) is currently a Professor and Dean of Faculty of Engineering and Applied Science at University of Ontario Institute of Technology (UOIT), Oshawa, ON, Canada.

Mohammad R. Dadash Zadeh (M’06) is currently working as manager of T&D protection division of ETAP-Operation Technology Inc, Irvine, CA, USA

Zhiying Zhang (M’94–SM’09) is currently a principal applications engineer with GE Grid Solutions, Markham, ON, Canada.